JMEPEG (2011) 20:1392–1400
DOI: 10.1007/s11665-010-9776-0

1059-9495/$19.00

Comparative Study of Several Energy Dissipating Devices

A. Abdul-Latif

(Submitted September 10, 2009; in revised form August 30, 2010)

Large plastic lateral collapse problem of two geometrically identical hollow cylinders under compressive load is of particular interest in this work, since, the energy absorbed can be characterized by a smooth loaded deflection relation, and these tubes are also easier to build than most other devices. Cylinders of various geometrical parameters (i.e., inside/outside diameter ratios: R = di/do ranging from 0 to 0.473) are used having the same cross-sectional area and length. Superplastic material used in this study has a considerably sensitivity to the quasi-static strain rate in the range of (10^{-5} to 10^{-3}/s). Hence, this material could be employed as a representative material to simulate the classical engineering material behavior under high strain rate. Comparative study of different structural situations is conducted using four energy dissipating devices designed and investigated by the author in previous works. They are: (1) two geometrically identical cylinders made of superplastic tin-lead alloy can freely expand along their sides and lengths; (2) two cylinders are the same as in (1) but not allowed to expand along their sides and lengths; (3) one cylinder is made from superplastic and the other made from steel and free to deform along its sides and length; (4) the same as in (3) but the cylinder is not allowed to expand along its sides and length. Based on the obtained experimental results, the features of each device in dissipating the energy during the large plastic collapse are investigated. It is concluded that the energy absorbed for a given system decreases with the increase of the R ratio. It is recognized that the highest absorbed energy is obtained in the constrained situation with deformable non-deformable compared to the other situations. Moreover, through the finite element simulations, the flow mechanism in each device is studied and compared to the experimental results.

Keywords energy dissipating device, lateral plastic collapse, strain rate effect, superplastic material

1. Introduction

Energy dissipating devices are important in mitigating the damage and thus improving crashworthiness and vehicular collisions. A number of literature surveys represent the state of the art in this field (e.g., Ref 1–5) giving detailed discussion of the techniques and theoretical aspects of different energy absorption devices. These mechanical devices and elements that can be used in this field depend on the large plastic deformation. In general, the common structural elements are wires, bars, frames, and tubes.

A focusing is made now on the tubular components, which can be plastically flattened due to lateral compression and can be laterally crushed under local loads. Under axial compressive loadings, these elements can be also axi-symmetrically buckled. A great deal of attention has been given in studying the energy absorption. Recently, axial crushing of circular and square or rectangular sectioned tubes under static and dynamic loading conditions has been performed by many research programs and was reviewed by Abramowicz and Jones (Ref 6), Jones (Ref 4), and Reid (Ref 7). Furthermore, these tubular structures can be plastically made to turn inside-out or outside-in, known as tube inversion. Hence, crushing (axially or laterally) of cylinders has received a great deal of attention in the contest of energy dissipating systems.

In general, whatever the employed devices, the related investigation aims to understand the deformation modes, then the energy absorption patterns and the resulting failure during collapse. For a given structure, this energy depends exclusively on main parameters: the magnitude, type and method of load application, strain rates, deformation or displacement patterns, and material properties. Thus, the plastic flow has to be correctly determined through experimental and numerical procedures to thoroughly understand the structure response during collapse.

In recent decade, renewed interest has been observed in the application of other concepts like honeycombs, foams, biaxial plastic buckling, etc. (e.g., Ref 8–11). Beside the mass efficiency of such materials, their mechanical characteristics in compression demonstrate that they can be considered as an excellent energy absorber offering, notably for the honeycombs and foams, an obvious plateau of almost constant force in the uniaxial compressive force-displacement curve (for example, Ref 12–14).

In the light of this fact, the adopted solutions focus on the design of passive energy absorbing systems, which are frequently based on engineering materials seeking always a high-specific energy absorption ratio. Moreover, passive energy absorption devices are designed to successfully work in predefined collision scenarios. An examination of the relevant literature reveals that tubular structures are efficient in absorbing energy (per unit weight) in comparison with other structural elements. In general, under uniaxial crushing, a desirable characteristic for these devices is to obtain a relatively constant

A. Abdul-Latif, Laboratoire d'Ingénierie des Systèmes Mécaniques et des Matériaux (LISMMA), Supméca, 3, rue Fernand Hainaut, 93407 St Ouen Cedex, France and Université Paris 8, IUT de Tremblay, 93290 Tremblay-en-France, France. Contact e-mail: aabdul@iu2t.univ-paris8.fr.

crushing force. The importance of the geometrical parameters of tubular structures has been recently studied in controlling the energy absorbed via the deformation mode (Ref 15). Nonetheless, under lateral loading conditions, a smooth load-deflection relation can characterize the energy absorbed, and these tubes, which are not affected by the load direction, are easier to build than most other devices.

In the present work, two geometrically identical cylinders of (R = di/do) ranging from 0 to 0.473 are compressed between two semi-cylindrical platens along their common tangent. The cylinders are produced by forward extrusion made from fine grains superplastic tin-lead alloy, which is rate sensitive material at very low rates of strain. Hence, this alloy could be employed as a representative material to simulate the behavior of rate sensitive engineering materials at high strain rate. Four different structural conditions for the title problem are investigated: (1) two geometrically identical cylinders of various (R) made of superplastic tin-lead alloy (deformable) can freely expand along their sides and lengths, referred to deformable-deformable (DD) free situation (open rig); (2) two cylinders are the same as in (1) but not allowed to expand along their sides and lengths, referred to as DD constrained situation (closed rig); (3) one cylinder is made from superplastic (deformable: freely expanded along its sides and length) and the other made from high carbon steel; referred to as deformable non-deformable (DND) free situation; (4) the same as in (3) but the cylinder is not allowed to expand along its sides and length; referred to as DND constrained situation. A series of tests is carried out for the previously mentioned situations at quasi-static strain rate in the range of (10^{-5} to 10^{-3}/s) in order to assess their load-deflection and energy absorption characteristics.

2. Experimental Procedure

Cylindrical specimens, either solid or hollow, of different (R) values made from superplastic tin-lead (61.9-38.1% by weight) alloy are produced by forward extrusion with about 80% reduction (see Fig. 1). All these different right circular specimens have almost the same cross-sectional area. The initial billet size of 56 mm diameter is always used to produce these cylinders. The extruded specimen lengths are systematically of 120 mm (for the open rig) and 60 mm (for the closed rig). To guarantee the material homogeneity, a length of 20 mm is always discarded from each end of cylinder after extrusion.

The hollow cylinders are produced using different bore of extrusion cylinders and different diameter mandrels. It is worth noting that, in the case of hollow cylinder production, the initial billets have to be drilled, before achieving the extrusion process, according to the mandrel's diameter value. The reduction ratio, in the solid case (di/do = 0), is of 81%, while in the second extremity case (di/do = 0.473), the reduction represents 80%. Thus, the maximum deviation cannot exceed 1% leading almost, as it is assumed, to the same material properties. The final dimensions of the employed cylinders are reported in Table 1. Tests are carried out using special rigs. Actually, Fig. 2(a) represents the special rig used in the free situation (open rig). Displayed in Fig. 2(b), the general arrangement of the closed rig is used for the constrained type tests. They are conducted, for each case of R, on an Instron Universal Testing Machine at six constant cross head speeds,

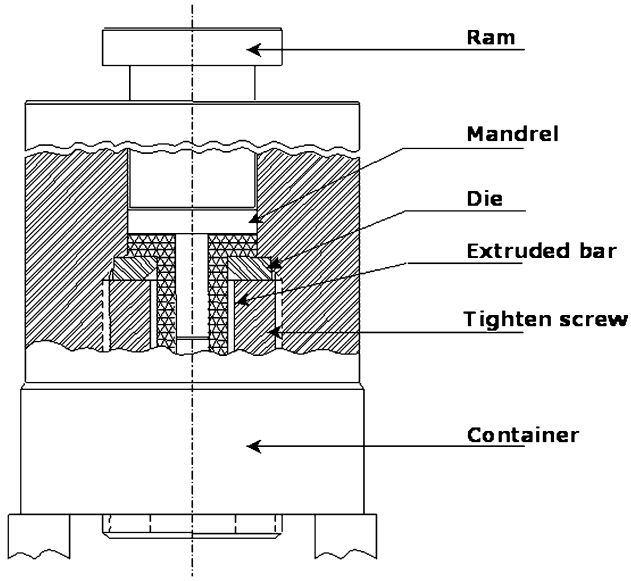

Fig. 1 Sectioned view of the extrusion apparatus

Table 1 Dimensions of tested cylinders

No.	(do), mm	(di), mm	di/do (R)	Length l_0, mm	Volume, mm^3
1(a)	24.4	0	Solid	120	56111.56
2	24.7	2.5	0.1	120	56910.57
3	24.9	5.08	0.204	120	56002.37
4(a)	25.5	7.2	0.283	120	56398.81
5	25.7	7.71	0.3	120	56647.24
6(a)	26.1	9.1	0.348	120	56397.87
7	27.2	11.7	0.43	120	56826.69
8(a)	27.7	13.1	0.473	120	56141.51

(a) Cylinders are used in the case of closed rig with length being of 60 mm

namely, 0.2, 0.5, 2, 5, 10, and 20 mm/min at room temperature. In order to ensure the experimental results accuracy, each test is repeated twice under the same experimental conditions (applied speed and temperature). If the difference between the two responses exceeds 3%, then another test has to be performed. Figure 3(a)-(d) shows some selected load-deflection behaviors of the four used energy dissipating devices. Experimentally, the energy absorbed at any corresponding deflection is also determined as shown in Fig. 4.

3. Results and Discussion

Let us now discuss the adopted experimental methodology and the different obtained results in studying the specimen geometry and the loading rate effects on the energy absorption for all mentioned cases (Table 1).

In order to describe the specimens response notably their plastic flow mechanisms, resorting to non-linear finite element represents an accurate way justified by many research programs. It is important to mention that for the finite element

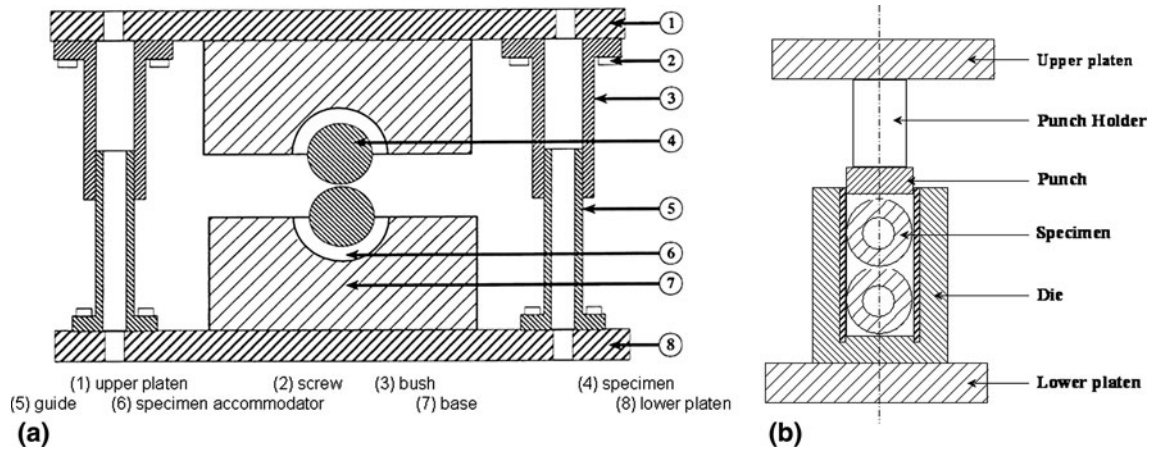

Fig. 2 Sectioned views of the assembled rigs of the (a) free situation (open rig) and (b) constrained situation (closed rig)

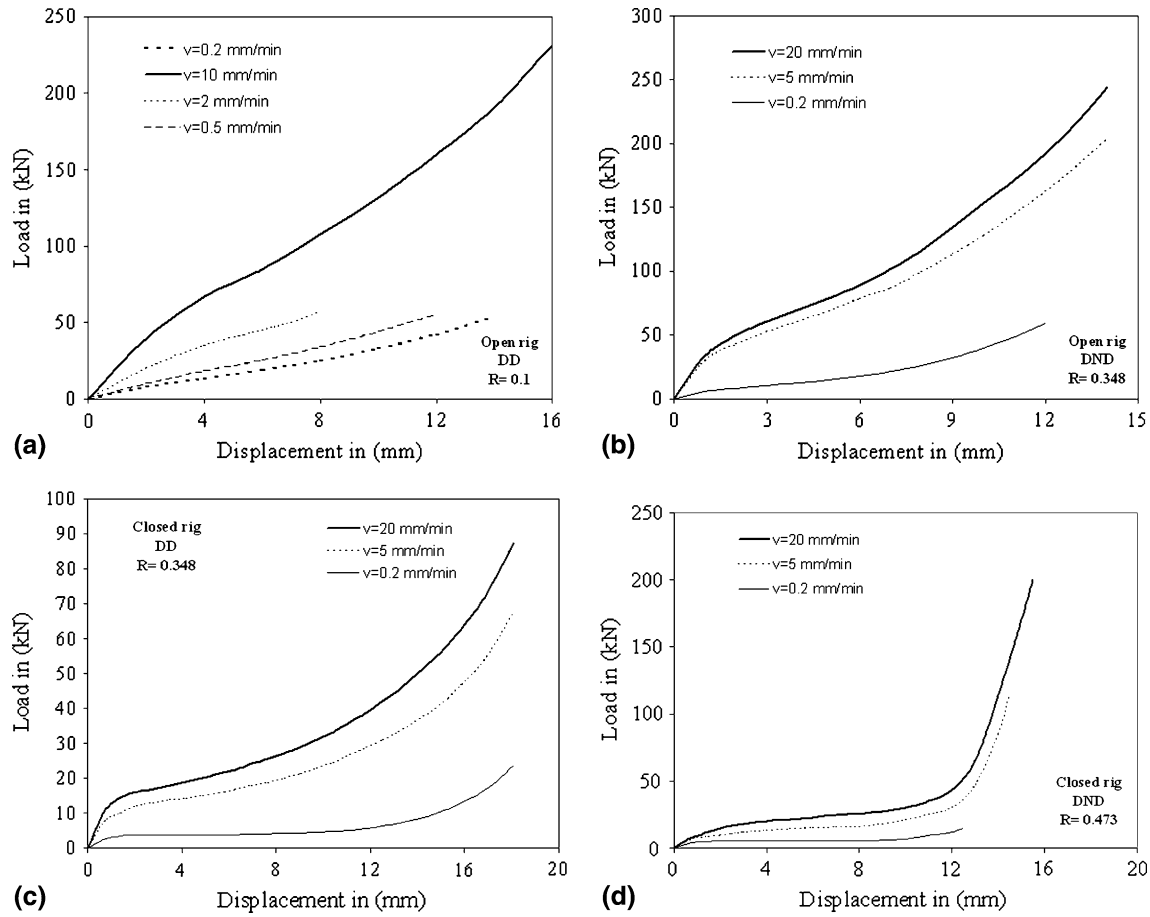

Fig. 3 Load-deflection characteristics at different strain rates in the DD and DND situations for different geometrical specimens and in the case of open and closed rigs

analysis, based on the geometrical symmetry, only one-half part of the specimen is descritized with six-node elements. Each rig is modeled as a rigid surface (Ref 16, 17) using the Norton-Hoff's law to reproduce the main phenomena encountered in such process. In fact, it is well-known that in the Norton-Hoff law of viscoplasticity, the stress is a function of the rate of permanent strain, i.e., the deformation of the material depends on the rate at which loads are applied. The inelastic behavior that is the subject of viscoplasticity is plastic deformation which means that the material undergoes unrecoverable deformations when a load level is reached. Note that the effect of elasticity is neglected in the model $\varepsilon_e = 0$ and hence there is no initial yield stress, i.e., $\sigma_y = 0$. Moreover, according to the constitutive law, the superplastic material is assumed to be homogeneous,

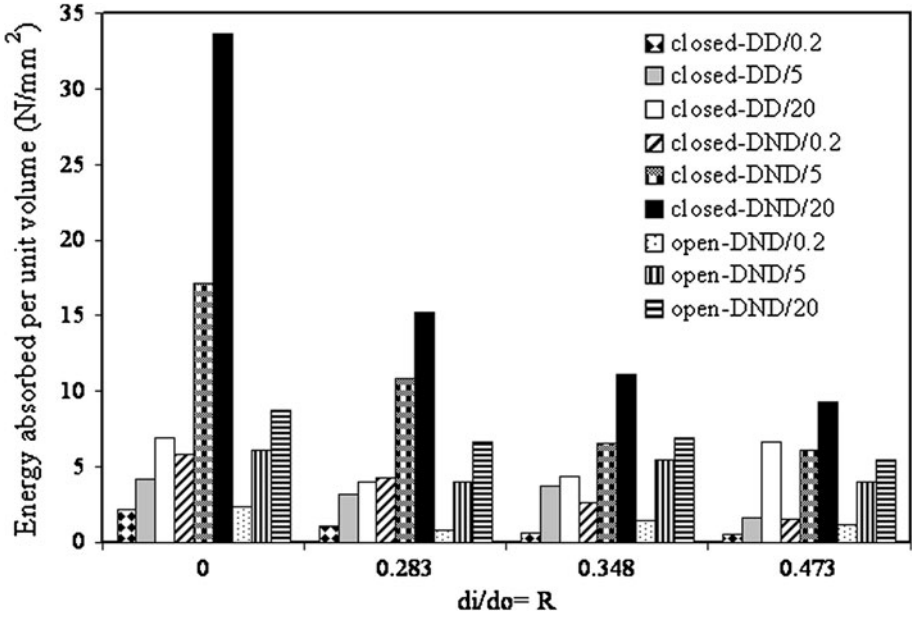

Fig. 4 Effect of R ratio on the energy absorbed per unit volume for the DD and DND situations in the case closed and open rigs at three loading rates for δ = 10 mm

isotropic, and incompressible. The following condition either on the velocity filed **v** or on the strain rate tensor $\mathbf{D} = \frac{1}{2}(\text{grad}^{t}(\mathbf{v}) + \text{grad}(\mathbf{v}))$ is added:

$$\text{div}(\mathbf{v}) = \text{tr}(\mathbf{D}) = 0 \qquad \text{(Eq 1)}$$

The elastic strain is negligible with respect to the irreversible (inelastic) strain and has a little effect on the material flow. The inelastic flow law of the Norton-Hoff type is often used in the following form:

$$\boldsymbol{\sigma} = 2K((\sqrt{3}\bar{d})^{m-1}\mathbf{D}, \qquad \text{(Eq 2)}$$

where **σ** is the Cauchy stress tensor which coincides with its deviatoric part, $\bar{d} = \sqrt{2/3\,(\mathbf{D}:\mathbf{D})}$ is the effective strain rate, K is the material consistency, and m is the strain rate sensitivity index. The two parameters have been already calibrated for the used material (Ref 18) giving 180 MPa for K and 0.4 for m. The expression of the employed law involving large deformation, does not pose the problem of the material frame indifference. It has an objective form since it does not introduce stress rate. The 2D finite element commercial code (FORGE2) is used with a rigid-viscoplastic model, where the stress is expressed in terms of strain rates. The approach is based on an updated Lagrangian description, where the geometry is fixed in each time step while equilibrium is iteratively solved. The geometry is then updated based on the calculated nodal velocities. The numerical simulation leads evidently to a highly distorted mesh due to the large deformation of the material. When the final topology is very different from the initial one, the same mesh topology is generally not convenient for the whole process. For these reasons, remeshing (available in used software) becomes mandatory and takes frequently place. Therefore, a new mesh is automatically generated as soon as one of the following criteria is reached: (i) distortion of a finite element or a segment of the boundary; (ii) bad description of the rig-part interface; (iii) large curvature of the segments of the free boundary and finally (iv) detection of a fold. The frictional less condition at the interface between the rig and cylinders is defined through some performed simulations compared to the experimental results. For further discussion about the theoretical and the practical aspects, the reader is referred to the Ref (16, 17).

The influence of the geometrical parameters, loading rate, and the structural situations (DD and DND) has been numerically investigated in Abdul-Latif and Nesnas (Ref 17). Several important features have been also studied for the structural situations such as: (i) non-homogeneous deformations; (ii) variable regions of contact between deformed cylinders and rig; (iii) the variation of the strain rate at material points; and (iv) rapid rise of total rig force when an important part between the cylinders and the rig is in contact.

3.1 Load-Deflection Behavior

As a typical example, Fig. 3 shows the force evolution during the lateral collapse of cylinders for the two employed rigs: the open and the closed rigs for the two structural situations (DD and DND). In fact, whatever R ratio and the loading rate values, three distinct phases of force evolution during the plastic collapse are recorded; first, for a small deflection (δ), the compressive force evolves rapidly with δ. Then, in the second phase, this evolution slows down for certain range of δ. This is due to the equilibrium between the increasing of the flattened area in the free deformation region between the two cylinders (outer cylinder halves, see Fig. 2a) and the relative decreasing of the strain rate. The deformation regions in the closed rig represent the contact region between the two cylinders and between each cylinder and the walls of the rig (Fig. 2b). Contrary to the second phase, the force evolves rapidly with δ in the third phase. In fact, this phenomenon can be interpreted by the fact that for a relatively high value of δ, the strain rate reaches practically its steady state, while the cylinders continue to be flattened in the deformation zone, giving a large area of contact and hence high frictional stresses, during which the sudden change in force evolution is attributed (Fig. 3). Whatever the value of R, this

behavior is obviously observed at the highest loading rate. The curves diverge with increasing deflection due to the change in the strain rate, reflecting the material sensitivity to strain rate. In addition, it is noticed that the deflection increases with an increase in the R ratio for a given force. In conclusion, at any particular load and structural condition, the deformation increases as the R ratio is increased. Similarly, as the loading rate increases, the required load is also increased at any particular deflection.

3.2 Effect of Loading Rate and Cylinder Geometry on the Energy Absorbed

As in Abdul-Latif (Ref 18), Nesnas and Abdul-Latif (Ref 16), and Abdul-Latif and Nesnas (Ref 17), the geometrical parameter of the cylinder (R = di/do) plays a considerable role in dissipating the energy for the developed devices. In order to examine the cylinder responses for the different structural situations, R ratios and loading rates, the energy absorbed per unit volume is recorded for an axial deflection of 10 mm. In fact, an examination of Fig. 4 reveals that the energy absorbed decreases with the increase of the R ratio for a given system and loading rate. Since the case of DD in the open rig has the smallest energy absorption capacity, therefore only the other three structural situations are presented in this comparison through Fig. 4. Furthermore, it points out that the relationship between the energy absorbed and R ratio is almost of similar pattern under the loading rates of 5 and 20 mm/min, where the effect of changing R on the absorbed energy is steeper. However, under a loading rate of 0.2 mm/min, the behavior of cylinders is different, i.e., the absorbed energy has a lower sensitivity to the R value compared to the above cases. Actually, this is due to the fact that the superplastic materials are more sensitive to strain rate at a range of 10^{-4} to 10^{-3}/s. This is in agreement with previous results (Ref 19).

Each of the four structural situations behaves in different way depending on the R ratio and the loading rate. In the open rig, the absorbed energy in the case of DD is mainly dissipated in flattening the cylinders in the common tangent between the cylinders (Ref 18). However, in the closed rig, it is mainly consumed in flattening the cylinders in the tangent region between the two cylinders, and at the constraining rig walls level and in the radial flow. The latter causes the closure of the bore. On the other hand, in the DND free situation, the deformation mode is rather complex, and in addition to the energy consumed in the flattening and bore closure; part of the energy is absorbed in indentation and flattened of the cylinder around the non-deformable cylinder and in the plastic flow along the length and horizontal diameter. In the DND constrained situation, the energy consumed in plastic collapse along the length and horizontal diameter is eliminated and replaced by the flattening and friction at the constrained walls. It appears at this point therefore that the constrained situation is advantageous to the free situation as shown through the histograms of Fig. 4, i.e., the energy consumed in the plastic flow along the length and horizontal diameter is less important than that consumed in flattening at the constrained walls. As a typical example (Fig. 4), for an axial deflection of 10 mm and R = 0 at 20 mm/min loading rate, the absorbed energies per unit volume are 33.7, 6.94, and 8.7 N/mm^2 for DND (closed rig), DD (closed rig), and DND (open rig), respectively, giving corresponding enhancements of 387 and 286% vis-à-vis the DD (closed rig) and DND (open rig). Less important differences are recorded in the case of hallow cylinders of R = 0.348 giving absorbed energies per unit volume of 11.1, 4.37, and 6.92 N/mm^2 for DND (closed rig), DD (closed rig), and DND (open rig), respectively. The corresponding increases are 153 and 60% in comparison with the DD (closed rig) and DND (open rig). Therefore, the DND constrained situation has the highest energy absorption capacity among the other systems.

3.3 Deformation Mode

In order to thoroughly understand the structure responses during the lateral crushing process, the resorting to the finite element method represents an accurate approach to determine the plastic flow mechanism. In the finite element analysis, the rig is modeled as a translating rigid surface. The identical pair of cylinders is intensively deformed at the tangential region [free deformation region between the two cylinders (outer cylinder halves)]. Since the treated problem consists of a large deformation configuration using a superplastic material as a deformed and representative material, the role of the elastic strain with respect to the inelastic one can therefore be neglected as in many other research programs. As a result, this material is modeled, via the Norton-Hoff law, as a rigid-viscoplastic material. Certainly, if the non-deformable cylinder is modeled as a deformable solid, the solution will be more accurate and rigorous. For the sake of simplicity, this cylinder is, however, modeled as a rigid body notably in the case of DND. This is also due to the fact that the elastic strain has a trivial role which can be neglected to reasonably resolve this problem as given in Nesnas and Abdul-Latif (Ref 16) and Abdul-Latif and Nesnas (Ref 17).

To model the contact between two deformable cylinders, the following procedure is conducted. At time t, if the node is already in contact with the die, two cases have to be considered: (1) the normal stress is compressive at time t and the node n remains therefore in contact. However, if the tool is not planar in the vicinity of the node n, a reprojection on the die will be again necessary; (2) the normal stress is no longer compressive, the point is then allowed to loose its contact with the die.

As far as the remeshing is concerned, with an updated Lagrangian formulation, the nodes of the mesh follow the kinematic evolution of the material points. This method leads to a highly distorted mesh due to the large deformation of the material. Moreover, when the final topology is very different from the initial one, the same mesh topology is generally not convenient for the whole process. For these reasons, remeshing is mandatory, and takes place frequently in some examples (it can be more than 300). Therefore, a new mesh is automatically generated as soon as one of the following criteria is reached: (1) distortion of a finite element or a segment of the boundary; (2) bad description of the die-part interface; (3) large curvature of the segments of the free boundary and finally (4) detection of a fold. For example, in the case where a fold is detected, the overlapping part of the domain is then removed from the boundary description before the mesh regeneration. This leads to some volume losses, but this simple procedure makes the simulation possible to continue giving satisfactory results (Ref 16).

The geometry of the undeformed mesh of the cylinders is shown in Fig. 8 assuming that there is one plane of symmetry. Accordingly, only one-half of the specimen is modeled with a six-noded triangular plane strain element. The number of elements used is varying according to the treated case

(233-392) and the number of calculations steps is 267-346. A number of remeshings has to be performed automatically because of severe mesh distortions occurring at the tangential region for the solid cylinders producing flattening and around the bore for the hollow ones. In addition, the fold detected at the contact between the two cylinders increases the relative density values of meshes to 68-87 in order to remove the overlapping part. Moreover, the friction between the specimen and the die is not experimentally characterized. However, repeated simulations with different friction coefficient values give no significant difference on the obtained load-deflection curves. The rest of simulations are then performed in the frictionless case.

As shown in Nesnas and Abdul-Latif (Ref 16), for the DD in the open rig, the distribution of the plastic strain in the tangential region between the two cylinders is demonstrated in Fig. 5 for the solid ($R = 0$) and hollow cylinders ($R = 0.473$). It points out the deformed finite element mesh of the solid specimen after 10 mm and hollow specimen after 13 mm of axial deflection. Some differences in the flow mechanism are recorded. In fact, it is shown that the flow mechanism is different for these cylinders. In fact, for the solid specimen, a zone of intense plastic flow is observed in the flattened region during the compressive loading. Moreover, a "dead zone" with less plastic strain is pointed out in the two semi-cylindrical parts under the accommodator (Fig. 5a, b). For the hollow specimen ($R = 0.473$), the two semi-cylindrical parts under the accommodator suffer from a more important plastic strain than that in the first case. However, its intensity remains distinctly lower than that in the tangential region and around the bore. In fact, the flow mechanism which develops toward the bore direction undergoes plastic strain localizations as plastic hinges in the lateral extremities of the deformed bore (Fig. 5c, d). These plastic hinges are often observed in the crushing of the thin tube cases. Such results are in a good agreement with experimental observations reported in Abdul-Latif (Ref 18).

Concerning the DND in the open rig, Fig. 6 shows the finite element mesh for the specimens for $R = 0$ and 0.348. The deformed mesh of the cylinder with $R = 0.348$ is presented in Fig. 6(b). After a deflection of 6 mm, the deformed cylinder has acquired a shape, which agrees fairly well with the experimental one (Fig. 7). According to the deformed mesh (Ref 16), the elements in lateral bore region are highly distorted leading to plastic strain localization zones. At these zones, the element becomes severely distorted and leads to increasing the frequency of remeshing operation. For $R = 0.348$ and $\delta = 6$ mm, Fig. 7 shows that the bore is not completely closed, while at 10 mm its closure is completely terminated.

As far as the DND in the closed rig is concerned, studying the flow mechanism via four successive deformed states

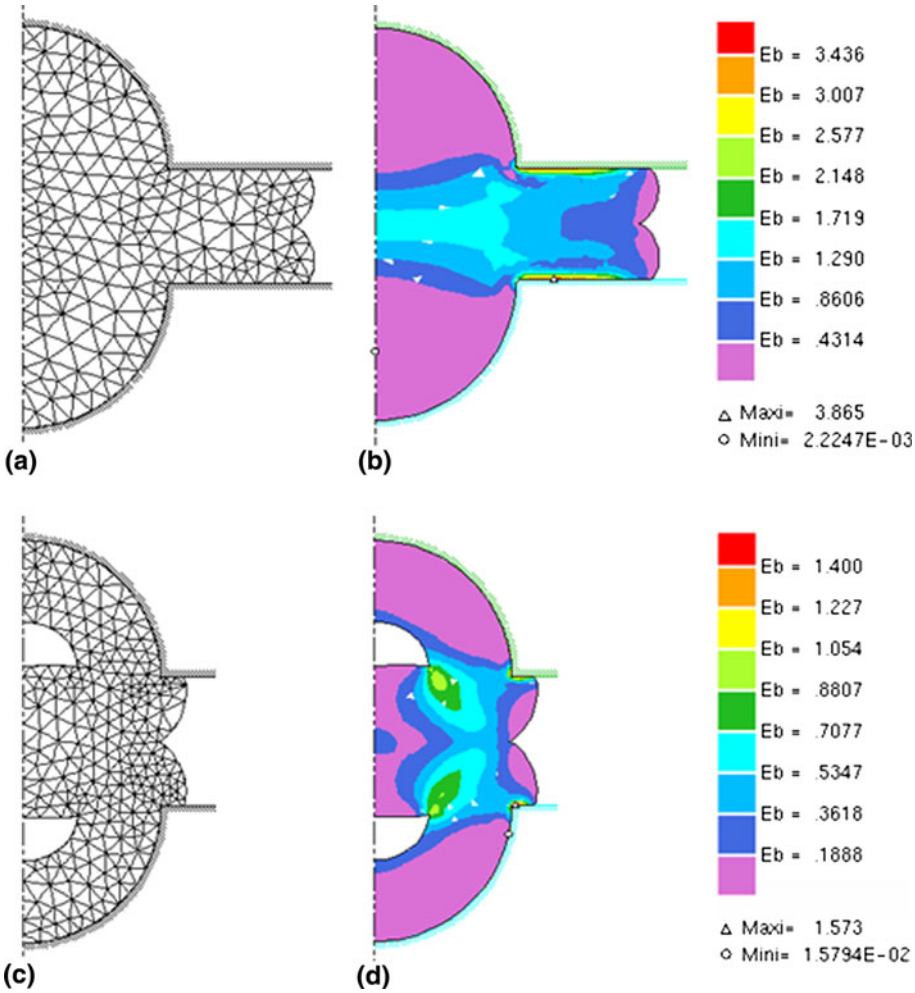

Fig. 5 Finite element plastic collapse simulations for the DD situation in the case of solid specimens ($R = 0$, for $\delta = 10$ mm) and hollow specimens ($R = 0.473$ for $\delta = 13$ mm): (a) and (c) finite element meshes, (b) and (d) plastic strain distributions

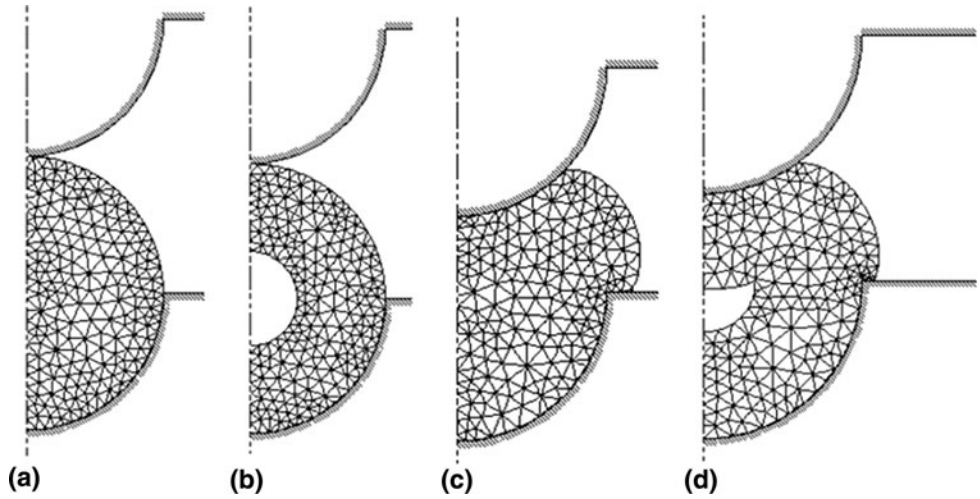

Fig. 6 Finite element meshes for the DND situation (a) for the solid cylinder, (b) for the hollow cylinder with $R = 0.348$, (c) deformed finite element mesh after 5 mm of axial deflection for the solid specimen, and (d) deformed finite element mesh after 6 mm axial deflection for hollow specimen having $R = 0.348$

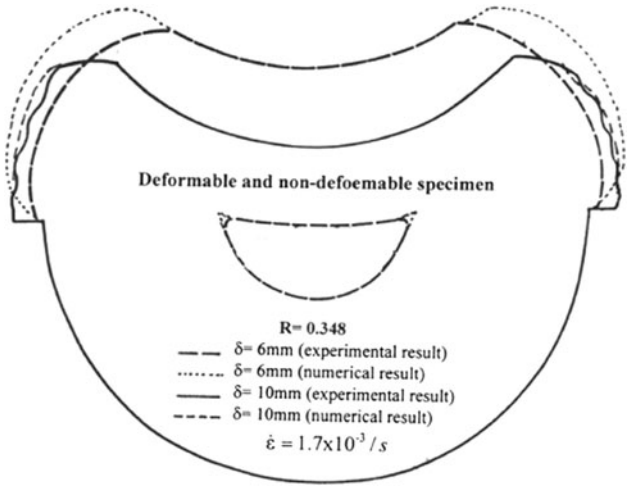

Fig. 7 Profiles of projected cross sections of hollow cylinders of $R = 0.348$ after different deformation levels in the DND situation (numerical and experimental comparison)

(for axial deflections: 4, 6, 8, and 10 mm) is presented in Fig. 8. It reveals a comparison between the experimental result and finite element prediction for these chosen deformed configurations. It demonstrates a progressive mechanism of the bore closure associated proportionally with the amount of the axial displacement at the loading rate of 5 mm/min. Moreover, this figure shows that a bore closure occurs for $\delta = 10$ mm. Figure 9 and 10 display the non-deformed meshes in the DD and DND cases for the closed rig, respectively. Despite the adoption of the two-dimensional plane strain using the Norton-Hoff's law to reproduce the behavior of the structures, it appears that this assumption gives almost an acceptable prediction of the flow mechanism. As an example for $R = 0.348$, the accumulated plastic strain distribution is presented at different deflections in these figures. In spite of the difference between the DD and the DND situations in their plastic flow mechanisms, the cylinders in both cases, however, suffer from a plastic strain in their commune contact region less

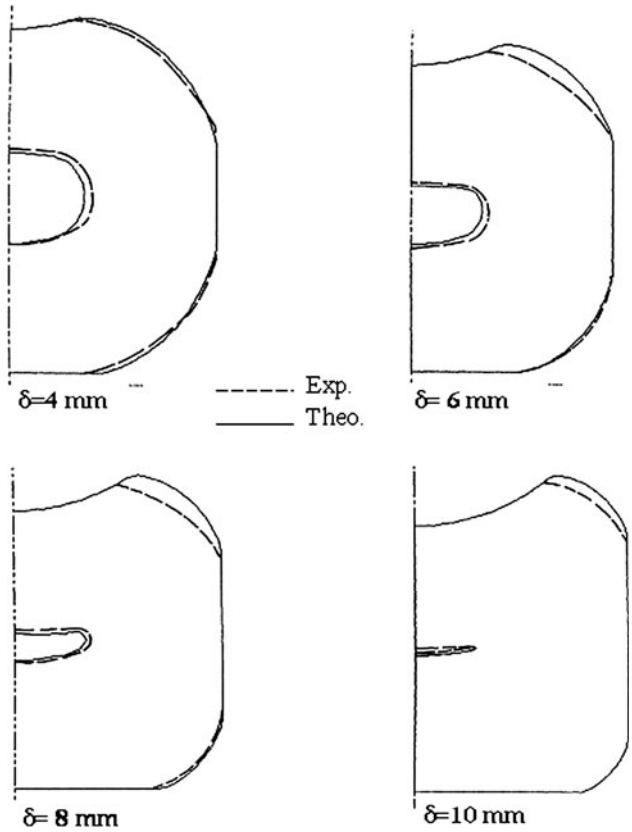

Fig. 8 Profiles of projected cross sections of hollow cylinders of $R = 0.348$ for different successive deformed states using the DND constrained situation (numerical and experimental comparison)

important than that in the zones around the bore (Fig. 9c and 10c). The flow mechanism that develops toward the bore direction undergoes plastic strain localization in the lateral extremities of the bore. Such zones are also observed above in the case of open rig. Hence, they can be considered as zones of damage initiation.

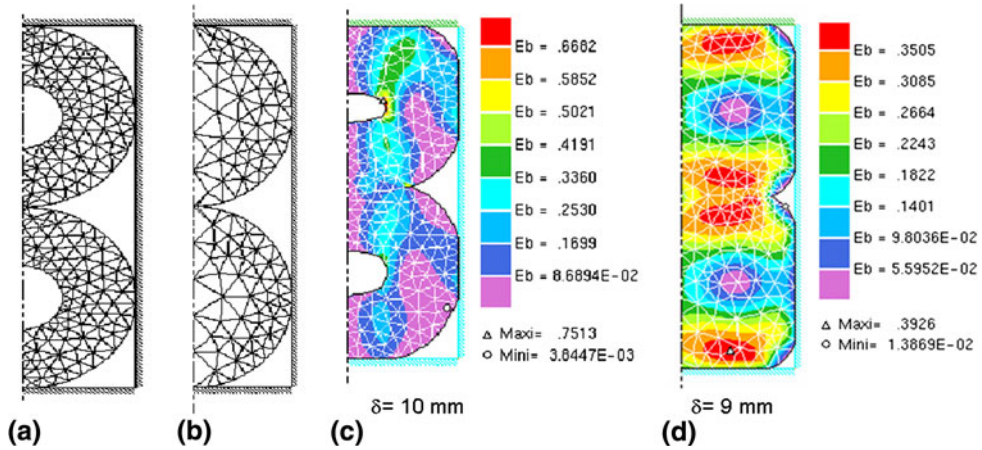

Fig. 9 Finite element meshes for the DD constrained situation: (a) $R = 0.348$, (b) $R = 0$; and plastic strain distributions for (c) $\delta = 10$ mm for $R = 0.348$ and (d) $\delta = 9$ mm for $R = 0.0$ at a loading rate of 5 mm/min

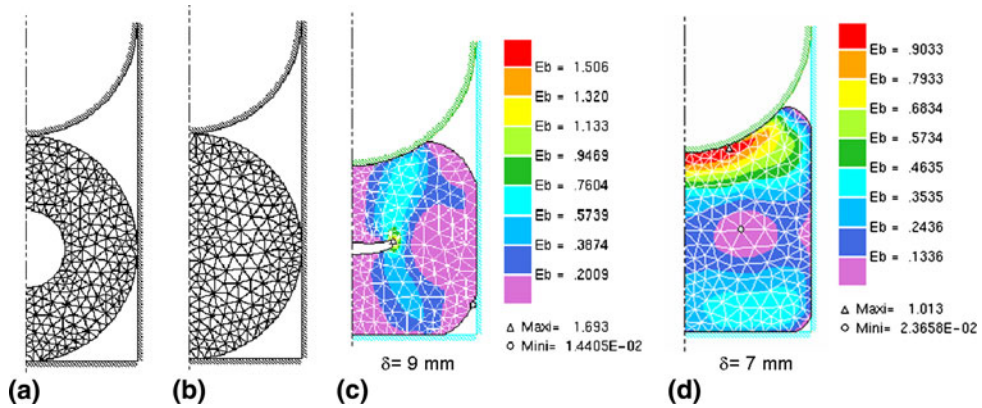

Fig. 10 Finite element meshes for DND constrained situation: (a) $R = 0.348$, (b) $r = 0$; and plastic strain distributions for (c) $\delta = 9$ mm for $R = 0.348$ and (d) $\delta = 7$ mm for $R = 0$ at a loading rate of 5 mm/min

In general, one can conclude that the non-linear finite element method describes fairly well the deformation mode under these different structural and loading rate conditions.

4. Conclusion

Designed and investigated in previous works, four energy dissipating devices study are used in this comparative. Such devices could be used for several engineering applications as a mean of absorbing energy and have a substantial role to play in the improvement of aircraft crashworthiness and vehicular collisions with the objective of minimizing human suffering and financial losses. They are (1) two geometrically identical cylinders made of superplastic tin-lead alloy can freely expand along their sides and lengths; (2) two cylinders are the same as in (1) but not allowed to expand along their sides and lengths; (3) one cylinder is made from superplastic (freely deformed along its sides and length) and the other made from steel; (4) the same as in (3) but the cylinder is not allowed to expand along its sides and length.

The experimental investigations show that the loading rate (strain rate) and the geometry of cylinders (R ratio) have a remarkable role on the plastic collapse mechanism and the absorbed energy whatever the rig type and the structural situation (i.e., DD or DND). The energy absorption capability increases with the loading rate increasing and the ratio R decreasing. Moreover, for these devices, the flow mechanism around the cylinder bore of the crushed cylinder is studied for a given loading rate showing successively the bore closure mechanism under different selected deflections.

This experimental study is supported by a numerical analysis based on the simple Norton-Hoff's constitutive equation as a model describing the plastic behavior of the loaded cylinders. In fact, the non-linear finite element method represents a useful and efficient tool to examine the plastic flow mechanism of the cylinders during their lateral plastic collapse. With this modeling, the flow mechanism of cylinders is successfully studied and compared with some experimental observations.

The type of the structural situation of cylinders (i.e., two deformable or DND cylinders) plays, for a given rig, a primordial role on the energy absorbed. Moreover, it is observe also that the rig type has a considerable influence on the amount of the dissipated energy. As a quantitative result, it is concluded that the DND in the closed rig has the highest energy absorption capacity among the examined systems.

References

1. A.A. Ezra and R.J. Fay, An Assessment of Energy Absorbing Devices for Prospective Use in Aircraft Impact Situations, *Dynamic Response of Structures*, G. Hermann and N. Perrone, Ed., Pergamon Press, Oxford, 1972, p 225–246
2. B. Rawlings, Response of Structures to Dynamic Loads, *Proc. Conf. on Mechanical Properties of Materials at High Rates of Strain*, Institute of Physics, 1974, p 279–298
3. W. Johnson and S.R. Reid, Update to Metallic Energy Dissipating Systems, *Appl. Mech. Rev.*, 1978, **31**, p 277–288 (*Appl. Mech.* Update 1986, p 315–319)
4. N. Jones, *Structural Impact*, Cambridge University Press, Cambridge, UK, 1989
5. A.A.A. Al-Ghamdi, Collapsible Impact Energy Absorbers: An Overview, *Thin-Walled Struct.*, 2001, **39**, p 189–213
6. W. Abramowicz and N. Jones, Dynamic Progressive Buckling of Circular and Square Tubes, *Int. J. Impact Eng.*, 1986, **4**, p 243–270
7. S.R. Reid, Plastic Deformation Mechanisms in Axially Compressed Metal Tubes Used as Impact Energy Absorbers, *Int. J. Mech. Sci.*, 1993, **35**, p 1035–1052
8. A.F. Bastawros, H. Bart-Smith, and A.G. Evans, Experimental Analysis of Deformation Mechanisms in a Closed-Cell Aluminum Alloy Foam, *J. Mech. Phys. Solids*, 2000, **48**, p 301–322
9. P.J. Tan, S.R. Reid, J.J. Harrigan, Z. Zou, and S. Li, Dynamic Compressive Strength Properties of Aluminum Foams: Part I—Experimental Data and Observations, *J. Mech. Phys. Solids*, 2005, **53**, p 2174–2205
10. A. Abdul-Latif and R. Baleh, Dynamic Biaxial Plastic Buckling of Circular Shells, *J. Appl. Mech.*, 2008, **75**, p 031013
11. R. Baleh and A. Abdul-Latif, Uniaxial-Biaxial Transition in Quasi-Static Plastic Buckling Used as an Energy Absorber, *J. Appl. Mech.*, 2007, **74**, p 628–635
12. A.G. Hanssen, M. Langseth, and O.S. Hopperstad, Static and Dynamic Crushing of Circular Aluminum Extrusions with Aluminum Foam Filler, *Int. J. Impact Eng.*, 2000, **24**, p 457–507
13. A.M. Harte, A.F. Norman, and M.F. Ashby, Energy Absorption of Foam-Filled Circular Tubes with Braided Composites Walls, *Eur. J. Mech. A/Solids*, 2000, **19**, p 31–50
14. S.L. Lopatnikov, B.A. Gama, M.d.J. Haque, C. Krauthauser, and J.W. Gillespie, Jr., High-Velocity Plate Impact of Metal Foams, *Int. J. Impact Eng.*, 2004, **30**, p 421–445
15. A. Abdul-Latif, R. Baleh, and Z. Aboura, Effect of Plastic Flow Mechanisms on the Large Deformation of Hallow Tubes Loaded Axially, *Int. J. Solids Struct.*, 2006, **43**, p 1543–1560
16. K. Nesnas and A. Abdul-Latif, Lateral Plastic Collapse of Cylinders: Experiments and Modeling, *Comput. Model. Eng. Sci.*, 2001, **2**, p 373–388
17. A. Abdul-Latif and K. Nesnas, Plastic Collapse of Cylinders Under Constrained Sides and Length Conditions, *ASME J. Eng. Mater. Technol.*, 2003, **125**, p 215–221
18. A. Abdul-Latif, On the Lateral Collapse of an Identical Pair of Cylinders, *Int. J. Solids Struct.*, 2000, **37**, p 1955–1973
19. T.Y.M. Al-Naib and J.L. Duncan, Superplastic Metal Forming, *Int. J. Mech. Sci.*, 1970, **12**, p 463–477